



## Research paper

# Inhibitory effect of the recombinant *Phoneutria nigriventer* Tx1 toxin on voltage-gated sodium channels

Anita O. Silva<sup>a</sup>, Steve Peigneur<sup>b</sup>, Marcelo R.V. Diniz<sup>c</sup>, Jan Tytgat<sup>b</sup>, Paulo S.L. Beirão<sup>a,\*</sup>

<sup>a</sup> Dept. of Biochemistry and Immunology, Instituto de Ciências Biológicas, Universidade Federal de Minas Gerais – UFMG, Av. Antonio Carlos 6627, 31270-901 Belo Horizonte, MG, Brazil

<sup>b</sup> Laboratory of Toxicology, University of Leuven (KU Leuven), Campus Gasthuisberg, PO Box 922, Herestraat 922, B-3000 Leuven, Belgium

<sup>c</sup> Laboratório de Biologia Molecular, Centro de Pesquisa Carlos Ribeiro Diniz, Fundação Ezequiel Dias, Rua Conde Pereira Carneiro 80, 30.510-010 Belo Horizonte, MG, Brazil

## ARTICLE INFO

## Article history:

Received 13 May 2012

Accepted 20 August 2012

Available online 30 August 2012

## Keywords:

Sodium channel

Sodium current

Spider toxin

Peptide toxin

Sodium channel inhibition

Isoform selectivity

## ABSTRACT

*Phoneutria nigriventer* toxin Tx1 (PnTx1, also referred to in the literature as Tx1) exerts inhibitory effect on neuronal (Nav1.2) sodium channels in a way dependent on the holding potential, and competes with  $\mu$ -conotoxins but not with tetrodotoxin for their binding sites. In the present study we investigated the electrophysiological properties of the recombinant toxin (rPnTx1), which has the complete amino acid sequence of the natural toxin with 3 additional residues: AM on the N-terminal and G on the C-terminal. At the concentration of 1.5  $\mu$ M, the recombinant toxin inhibits Na<sup>+</sup> currents of dorsal root ganglia neurons (38.4  $\pm$  6.1% inhibition at –80 mV holding potential) and tetrodotoxin-resistant Na<sup>+</sup> currents (26.2  $\pm$  4.9% at the same holding potential). At –50 mV holding potential the inhibition of the total current reached 71.3  $\pm$  2.3% with 1.5  $\mu$ M rPnTx1. The selectivity of rPnTx1 was investigated on ten different isoforms of voltage-gated sodium channels expressed in *Xenopus* oocytes. The order of potency for rPnTx1 was: rNav1.2 > rNav1.7  $\approx$  rNav1.4  $\geq$  rNav1.3 > mNav1.6  $\geq$  hNav1.8. No effect was seen on hNav1.5 and on the arthropods isoforms (DmNav1, BGNv1.1a and VdNav1). The IC<sub>50</sub> for Nav1.2 was

brought to you by CORE

provided by Elsevier - Publisher Connector

a valuable model to achieve pharmacological activities of interest for the treatment of channelopathies and neuropathic pain.

© 2012 Elsevier Masson SAS. Open access under the Elsevier OA license.

## 1. Introduction

Sodium channels form a super family of membrane proteins specialized in electrical signaling and ionic homeostasis. These channels are highly selective for Na<sup>+</sup> ions and their probability of opening depends on membrane potential and time, what makes them key elements for the initiation and propagation of the action potential in excitable cells. Nine subtypes of mammalian voltage-dependent sodium channels were identified and characterized (Nav1.1–Nav1.9). Each isoform can be distinguished for its pharmacological properties and functional characteristics. More

importantly, many subtypes of sodium channels are specialized, so that specific blocking agents may alter some physiological functions while preserving others. Alterations in the activity or expression of voltage-gated sodium channel subtypes are associated with several pathological conditions such as epilepsy, stroke and neuropathic pain. Because of their high affinity and specificity, neurotoxins may be powerful tools to study ion channels, through the understanding of their mode of action and identification of their molecular binding sites to ion channel, and are potential models for the development new drugs [1–3].

Interesting biological activities can be found in animal venoms. Among them, the venom of the spider *Phoneutria nigriventer* has been shown to be a rich source of peptides with diverse biological activities [4,5]. In contrast, its drawback is that the amount of each toxin found in the venom is very low. Added to the fact that the volume of venom produced by each spider is small, it becomes difficult to purify and identify the structure and biological properties of each peptide.

Abbreviations: PnTx1, *Phoneutria nigriventer* toxin 1; rPnTx1, recombinant PnTx1; KIIIA,  $\mu$ -conotoxin KIIIA; GIIIA,  $\mu$ -conotoxin GIIIA; SIIIA,  $\mu$ -conotoxin SIIIA; TTX, tetrodotoxin; DRG, dorsal root ganglia; TEA, tetraethyl ammonium; Nav, voltage-gated sodium channel.

\* Corresponding author. Tel./fax: +55 31 3409 2663.

E-mail address: [pslb@ufmg.br](mailto:pslb@ufmg.br) (P.S.L. Beirão).

One way of overcoming this limitation is by heterologous expression of the toxic peptide. The expression of the *P. nigriventer* toxin Tx1 (PnTx1) was an important step to express cysteine-rich toxins [6]. The recombinant toxin (rPnTx1) has the complete amino acid sequence of the natural toxin with 3 additional residues: AM on the N-terminal and G on the C-terminal, and molecular mass of  $8858.10 \pm 0.33$  Da. It was shown to reproduce the neurotoxic symptoms of the native toxin: tail elevation, excitation, salivation and spastic paralysis, when administered by intracerebro-ventricular injection on mice [6,7]. PnTx1 has a molecular mass of 8594.6 Da, 78 amino acid residues, 14 of which are cysteines. Its inhibitory activity on sodium channels has been reported, with the important detail that the inhibition is enhanced by depolarization of the membrane [8]. An inhibitory effect on calcium channels had been reported previously [9,10]. This effect was later attributed to the presence of a very small contamination with PnTx3-3 [8], already described as a potent calcium channel inhibitor [11]. However, the possibility that it is a promiscuous toxin remained, because PnTx1 shares sequence similarity with other toxins known to inhibit calcium channels [5].

In the present work, we report for the first time the subtype and phyla selectivity of this unique and potent spider recombinant toxin, which has the following order of potency:  $rNav_{1.2} > rNav_{1.7} \approx rNav_{1.4} \geq rNav_{1.3} > mNav_{1.6} \geq hNav_{1.8}$ . No effect was observed on  $hNav_{1.5}$  and arthropod isoforms. Taking advantage that rPnTx1 is devoid of contamination with other toxins, we verified that it has no significant effect on  $Ca^{2+}$  currents. Given the maintenance of full activity of the recombinant toxin, the present work opens new promising perspectives to the study of structure–activity relationship and to engineering rPnTx1 in order to improve its selectivity by site-directed mutagenesis.

## 2. Materials and methods

### 2.1. Expression construct and protein expression

The protocol used is the same described by Diniz and colleagues [6] with modifications [12]. Briefly, the 250-bp DNA sequence encoding the mature PnTx1 was amplified by PCR using specific primers, sense 5'-AGAGAGACCATGGCCGAGTAAACGAGCTGC-3' and antisense 5'-GAGAGAGGATCCTTAGCAATTTCTCTGCAGGG-3' that included 5'*Nco*I and 3'*Bam*H1 restriction enzyme sites, respectively. The amplified product was cleaved with *Nco*I and *Bam*H1, ligated into similarly digested pET32c(+) and used to transform *Escherichia coli* NM22 cells and cultured into Luria–Bertani (LB) medium, containing 100  $\mu$ g/ml of ampicillin at 37 °C. The PCR selected clones were certified by DNA sequencing [13] using an automated DNA sequencer (ALFexpress DNA sequencer, Amersham Pharmacia Biotech) following the manufacturer's own protocol and reagents. Isolated expression construct was used to transform competent cells of *E. coli*, the expression host (AD494(DE3)pLysS). Individual clones were grown at 37 °C in LB medium containing 100  $\mu$ g/ml ampicillin and 34  $\mu$ g/ml chloramphenicol until  $A_{600}$  of approximately 0.5 (cell density of  $5 \times 10^8$  cells/ml). Cells were induced by the addition of isopropyl  $\beta$ -D-thiogalactoside (IPTG) to a final concentration of 1 mM. Cells were harvested 2–2.5 h after the addition of IPTG and the pellets were then frozen at –70 °C. Induced frozen cells were thawed and re-suspended in 5 mM imidazole, 0.5 M NaCl and 20 mM Tris–HCl, pH 7.9 (binding buffer) and the cells were lysed by sonication. After centrifugation, the supernatant containing soluble recombinant fusion protein was loaded onto Histrap™ HP Chelating affinity column (Amersham Biosciences, HPLC) charged with 500 mM NiSO<sub>4</sub> and equilibrated with binding buffer. Unbound proteins were eluted from the chelating column with binding buffer. Fusion

proteins were eluted with linear gradient of 500 mM imidazole, 0.5 M NaCl and 20 mM NaHPO<sub>4</sub>, pH 7.4 (elution buffer) and the fractions containing thioredoxin–rPnTx1 fusion protein were detected by PAGE-SDS 12.5% (w/v). The fractions containing thioredoxin–rPnTx1 fusion protein were pooled, further purified and desalted by gel filtration chromatography (Histrap™ HP Desalting, Amersham Biosciences, HPLC) and lyophilized. After cleavage with enterokinase (following the Novagen protocol), the products were subjected to reverse-phase chromatography (Sephasil Peptide C18 5 m ST 4.6/250; HPLC). The recombinant protein was detected by mass spectrometry MALDI-TOF analysis and used for biological tests.

### 2.2. Culture of rat dorsal root ganglia (DRG) neurons

Male Wistar rats (250–300 g) were maintained in a controlled environment (circadian cycle, 25 °C, food and water *ad libitum*), 2 animals in each cage. All procedures involving animals were in accordance with the guidelines provided by the regulations on ethics and animal experimentation of the Brazilian Government.

Neurons of DRG were dissociated and used as described previously [14]. The DRG were isolated and maintained in  $Ca^{2+}$ -free modified Ringer solution containing (in mM) NaCl 140, KCl 2.5, HEPES 10, and glucose 7.5, pH adjusted to 7.4 with NaOH. The enzymatic treatment was done with papain (1 mg/ml, Sigma), activated by cysteine (0.03 mg/ml, Sigma) in  $Ca^{2+}$ -free Ringer, followed by enzymatic treatment with 2.5 mg/ml collagenase (Type 1A, Sigma) in  $Ca^{2+}$ -free Ringer, for 20 min each one.

Digested ganglia fragments were suspended in 1 ml of F12 medium containing 10% fetal bovine serum (Cripion, São Paulo, Brazil) and dissociated by passing through fire polished pipettes (inner tip diameter of 2 mm). The cell suspension thus obtained was plated onto glass coverslips previously treated with poly-L-lysine (MW 70,000–150,000, 0.1% v/w, for 12 h at 4 °C) followed by laminin (20 mg/ml, for 6 h at 4 °C). The cells were stored for 2 h at 37 °C in a 5% CO<sub>2</sub> incubator. After this period, the medium was changed to L15 medium containing 10% fetal bovine serum, penicillin (100 units/ml) and streptomycin (100  $\mu$ g/ml). The cultures were stored at room temperature and used within 48 h.

### 2.3. Heterologous expression of sodium channels

The oocytes were surgically removed from anaesthetized adult female frogs *Xenopus laevis*. Stage V and VI oocytes were selected and injected with 50 nl of RNA at a concentration of 1 ng/nl using a micro-injector (Drummond Scientific, USA). For the expression, the  $rNav_{1.2}/pCLT1$ ,  $rNav_{1.3}/pNa3T$ ,  $rNav_{1.4}/pUI-2$ ,  $mNav_{1.6}/pLCT1$ ,  $hNav_{1.8}/pBSTA$ ,  $DmNav_{1}/pGH19$ ,  $BgNav_{1.1}/pGH19$  and  $VdNav_{1}/pGH19$  vectors were linearized with Not I. The  $rNav_{1.7}/pBSTA$ , and  $h\beta 1/pGEM-HE$  vectors were linearized with Sac II and Nhe I, respectively. These vectors were transcribed with the T7 mMESSAGE-mMACHINE transcription kit (Ambion). The  $hNav_{1.5}/pSP64T$  and  $r\beta 1/pSP64T$  constructs were linearized with Xba I and Eco RI, respectively, and transcribed with the SP6 mMESSAGE-mMACHINE transcription kit (Ambion). The oocytes were incubated in a solution containing (in mM): NaCl, 96; KCl, 2; CaCl<sub>2</sub>, 1.8; MgCl<sub>2</sub>, 2 and HEPES, 5 (pH 7.4), supplemented with 50 mg/l gentamycin sulfate and 180 mg/l theophylline.

### 2.4. Electrophysiology

#### 2.4.1. DRG neurons

Sodium currents were recorded using the patch clamp technique in the modality whole cell with an Axopatch 200B amplifier controlled by PClamp 6 software (Molecular Devices, Sunnyvale,

CA). Soft glass patch pipettes were made with a two-stage vertical pipette puller (PP 830 Narishige, Tokyo, Japan) and had resistances of 1.0–1.5 M $\Omega$ . The elicited currents were sampled at 10 kHz and filtered at 5 kHz using a four-pole low-pass Bessel filter. Pipette solution contained (in mM) CsF 100, NaCl 20, HEPES 10, EGTA 11, tetraethyl ammonium chloride (TEA-Cl) 10, MgCl<sub>2</sub> 5, pH 7.2 with CsOH. Whole-cell recording conditions were obtained at extracellular solution containing (in mM) NaCl 115, CaCl<sub>2</sub> 2, MgCl<sub>2</sub> 1, HEPES 10, TEA-Cl 20, CdCl<sub>2</sub> 0.2, NiCl<sub>2</sub> 0.2, glucose 5, pH 7.4 adjusted with NaOH. After establishing the whole-cell configuration, the bath solution was changed to one containing 30% (v/v) of the extracellular solution described above and 70% (v/v) Na-free extracellular solution containing (in mM) choline chloride 115, KCl 5, CaCl<sub>2</sub> 2, MgCl<sub>2</sub> 1, HEPES 10, TEA-Cl 20, CdCl<sub>2</sub> 0.2, NiCl<sub>2</sub> 0.2, glucose 5, pH 7.4 adjusted with choline hydroxide. The final extracellular Na<sup>+</sup> concentration was 34.5 mM.

Unless otherwise stated, the cell under examination was held at –80 mV and maintained under continuous perfusion, either with control or experimental solution. In order to elicit Na<sup>+</sup> currents, a pre-pulse of –100 mV was applied for 100 ms, to remove inactivation, and was followed by the test pulse, whose values and durations are shown in each figure. Leak subtraction was performed using a P/4 protocol. This protocol was carried out every 5 s.

For recording calcium currents, the pipette solution was (mM): CsCl 140, HEPES 10, ATP Li e creatine phosphate 10; pH 7.4 adjusted with CsOH. The external solution contained (mM): TEA-Cl 132, CaCl<sub>2</sub> 2, CsCl 4, HEPES 10, Glucose 11, MgCl<sub>2</sub> 1; pH 7.4 adjusted with TEA-OH. The holding potential utilized was –80 mV. In order to observe the effect of rPnTx1 on calcium currents, the test pulse was –20 mV for 200 ms.

#### 2.4.2. *X. laevis* oocytes

For electrophysiological experiments in oocytes, two-electrode voltage clamp recordings were performed at room temperature using a Gene Clamp 500 amplifier (Molecular Devices, Sunnyvale, California, USA) controlled by a pClamp10 data acquisition system (Molecular Devices). Voltage and current electrodes were filled with 3 M KCl. Resistances of both electrodes were kept between 0.5 and 1.5 M $\Omega$ . The elicited currents were sampled at 20 kHz and filtered at 2 kHz using a four-pole low-pass Bessel filter. The external solution consisted of (mM): NaCl 96, KCl 2, MgCl<sub>2</sub> 1, CaCl<sub>2</sub> 1.8, HEPES 5; adjusted to pH 7.5 with NaOH.

To evoke sodium current, standard voltage clamp protocols were used, from a holding potential of –90 mV and with 5 s interval between each test. Sodium current traces were evoked by 100 ms depolarization to 0 mV. The current–voltage relationships were determined by 50 ms step depolarizations between –90 and 70 mV, using 5 mV increments.

To analyze the voltage-dependence of activation, the sodium conductance ( $g_{Na}$ ) was calculated by linear regression of the ohmic segment of the current–voltage ( $I$ – $V$ ) relationship. Using the obtained parameters,  $I_{Na(max)}$  was calculated by extrapolation of the current to each potential. The fraction of channels activated was given by  $I_{Na}/I_{Na(max)}$ , where  $I_{Na}$  is the measured peak Na<sup>+</sup> current and  $I_{Na(max)}$  is the expected current if all channels were open. The data were fitted to a Boltzmann equation:  $I_{Na}/I_{Na(max)} = 1/[1 + (\exp(V_g - V_p)/k_g)]$ , where  $V_g$  is the voltage corresponding to half-maximal conductance,  $V_p$  is the test pulse potential and  $k_g$  is the slope factor.

Toxin-induced effects on the steady-state inactivation were investigated using a standard two-step protocol. In this protocol, 200 ms conditioning pre-pulses ranging from –90 to 65 mV (with 5 mV increments) were followed by a 100 ms test pulse to 0 mV. Data were normalized to the maximal Na<sup>+</sup> current amplitude ( $I_{max}$ ), plotted against the pre-pulse potential and fitted using the

Boltzmann equation:  $I_{Na}/I_{max} = 1/[1 + \exp((V_c - V_h)/k_h)]$ , where  $V_h$  is the voltage corresponding to half-maximal inactivation,  $V_c$  is the conditioning pre-pulse voltage and  $k_h$  is the slope factor.

#### 2.4.3. Data analysis

For dose–response graphics, we used the simple rectangular hyperbolic equation:

$y = \max * c / (IC_{50} + c)$ , where max is the maximum effect,  $c$  is the toxin concentration and  $IC_{50}$  is the concentration that produces half-maximal effect.

Curve-fitting was achieved using Sigma Plot software. Data are presented as mean  $\pm$  SEM in the text and in the figures. Results were analyzed using Student's paired  $t$  test. Unless otherwise stated, differences were considered statistically significant when  $P < 0.05$ .

### 3. Results

#### 3.1. Effect of recombinant toxin in DRG neurons

Our first step was to check the effect of recombinant toxin in DRG neurons. Among the population of neurons found in the dissociated ganglia, cells with smaller diameters are an interesting model for experimental studies since they express both tetrodotoxin-sensitive sodium channels (TTX-S) ( $Na_v1.1$ ,  $Na_v1.2$ ,  $Na_v1.6$  and  $Na_v1.7$ ) and TTX-resistant channels (TTX-R) ( $Na_v1.8$  and  $Na_v1.9$ ) [15,16], and are involved in the transmission of pain signals to the central nervous system [16]. Fig. 1A shows the typical inhibitory effect of 3  $\mu$ M rPnTx1 on Na<sup>+</sup> currents of DRG neurons. In order to verify the toxin effect on TTX-R currents, DRG neurons were perfused with external solution containing 300 nM TTX, which is enough to inhibit TTX-S currents, and subsequently perfused with the same solution to which rPnTx1 was added. The effect of 3  $\mu$ M rPnTx1 is shown in Fig. 1B. At the concentration of 1.5  $\mu$ M, the average inhibition of rPnTx1 was  $38.4 \pm 6.1\%$  and  $26.2 \pm 4.9\%$  on total and on TTX-R Na<sup>+</sup> currents, respectively. The concentration-dependence of the inhibitory effect on DRG Na<sup>+</sup> currents is shown in Fig. 1D. The results were fitted with the rectangular hyperbolic equation (Material and methods) and the best fit was obtained with the  $IC_{50}$  of 0.6  $\mu$ M and maximal inhibition of  $44.2 \pm 5.6\%$ .

In order to investigate if the effect of the recombinant toxin is dependent on the state of the channel, Na<sup>+</sup> currents were elicited in cells with holding potential of –50 mV. The same pulse protocol was used, including the conditioning 100 ms pre-pulse to –100 mV. The inhibitory effect of 1.5  $\mu$ M rPnTx1 is shown in Fig. 1C. With this protocol, the percentage of inhibition at 1.5  $\mu$ M rPnTx1 was  $71.3 \pm 2.3\%$ . For comparison, this result is shown in Fig. 1D (open symbol).

#### 3.2. rPnTx1 effect on different $Na_v$ channel isoforms

To determine the phyla and subtype selectivity of rPnTx1, it was subject of an extensive study on a wide panel of 10 different isoforms of  $Na_v$  channels. Fig. 2 shows that this toxin exerts greater effect on  $Na_v1.2$  channels: at the concentration of 1  $\mu$ M the toxin could inhibit  $83.3 \pm 1.9\%$  of the sodium current through these channels. Higher concentrations of toxin could not increase the percentage of inhibition, suggesting that it attained a saturating concentration. Interestingly, the residual current could be blocked with 100 nM of TTX (data not shown). This phenomenon has been shown by Martin-Moutot and colleagues [8] using the natural toxin. Although with lower affinity, rPnTx1 could also inhibit  $Na_v1.3$ ,  $Na_v1.4$  and  $Na_v1.7$  with similar potencies ( $54.3 \pm 5.9\%$ ,  $63.2 \pm 5.3\%$  and  $65.4 \pm 4.8\%$ , respectively).  $Na_v1.6$  and  $Na_v1.8$  were

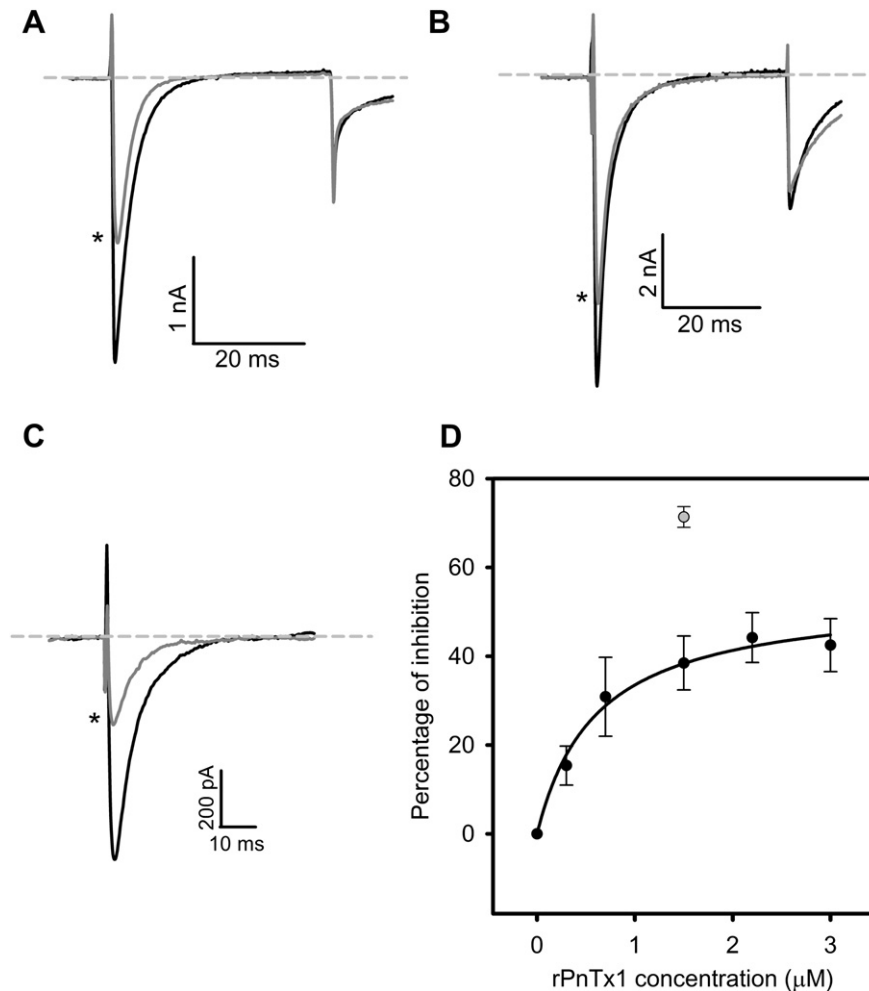


**Fig. 1.** Effect of rPnTx1 on  $\text{Na}^+$  currents of DRG neurons. (A) Representative  $\text{Na}^+$  currents before (black line) and 10 min after (gray line\*) the addition of 3  $\mu\text{M}$  rPnTx1. Holding potential:  $-80$  mV. (B) Representative TTX-resistant  $\text{Na}^+$  currents before (black line) and 10 min after (gray line\*) the addition of 3  $\mu\text{M}$  rPnTx1. Holding potential:  $-80$  mV. (C) Representative experiment on cell held at  $-50$  mV.  $\text{Na}^+$  currents before (black line) and 10 min after (gray line\*) the addition of 1.5  $\mu\text{M}$  rPnTx1. (D) Concentration–response relationship. Closed symbols, holding potential  $-80$  mV; open symbol, holding potential  $-50$  mV. Data were fitted using the rectangular hyperbolic equation shown in [Material and methods](#). Best fit was achieved with  $\text{max} = 44.2 \pm 5.6\%$  and  $\text{IC}_{50} = 0.6$   $\mu\text{M}$ . In all experiments the test pulse potential was  $-10$  mV.

less sensitive for this toxin since 1  $\mu\text{M}$  rPnTx1 could only inhibit a small percentage of the current ( $32.8 \pm 4.3\%$  and  $26.6 \pm 8.2\%$ , respectively). Interestingly, rPnTx1 was not significantly active on  $\text{Na}_v1.5$ , even at concentrations up to 5  $\mu\text{M}$ .

Similarly, rPnTx1 was also inactive on several arthropod  $\text{Na}_v$  channel isoforms. At 1  $\mu\text{M}$  the toxin failed to decrease the current peak amplitude of sodium channels from the following arthropods: fruit fly *Drosophila melanogaster* ( $\text{DmNa}_v1$ ), cockroach *Blattella germanica* ( $\text{BgNa}_v1.1a$ ) and mite *Varroa destructor* ( $\text{VdNa}_v1$ ) ([Fig. 2](#)).

### 3.3. Analysis of the effect of rPnTx1 on activation and inactivation of $\text{Na}_v1.2$

As pointed out, rPnTx1 has a higher affinity to  $\text{Na}_v1.2$  subtype. Therefore we used this isoform to further investigate whether the rPnTx1 induced inhibition is caused by altering the voltage-dependence of channel gating. [Fig. 3A](#) shows the current–voltage relationship in the presence and absence of 20 nM rPnTx1. There is a marked decrease of the peak current and maximum conductance to  $\text{Na}^+$  without significant change in the voltage dependence. This is better explored in [Fig. 3B](#), that shows no significant difference between the  $V_g$  of activation control conditions

( $V_g = -26.78 \pm 0.28$  mV) and after the addition of 1  $\mu\text{M}$  rPnTx1 ( $V_{1g} = -26.32 \pm 0.43$  mV). [Fig. 3C](#) shows no significant shift in the midpoint of the voltage-dependence of the steady-state inactivation caused by rPnTx1.

### 3.4. Comparison of the potency of the native and recombinant toxins

Since the recombinant toxin was produced in bacteria and has its amino acid sequence slightly modified, it is important to verify whether it retains the same effectiveness of the native toxin. Native PnTx1 purified as previously described [7] was used. Both peptides could inhibit  $\text{Na}_v1.2$  channels with the same efficacy (maximal inhibition of PnTx1:  $85.0 \pm 0.8\%$ ; rPnTx1:  $83.3 \pm 1.9\%$ ). Interestingly, the  $\text{IC}_{50}$  of recombinant toxin ( $\text{IC}_{50} = 33.7 \pm 2.9$  nM) was slightly but significantly lower than the  $\text{IC}_{50}$  of native toxin ( $\text{IC}_{50} = 105 \pm 12$  nM) ([Fig. 4](#)).

### 3.5. Effect of rPnTx1 in $\text{Na}_v1.2$ channels devoid of fast inactivation

In order to investigate if the action of rPnTx1 might be through stabilizing the inactivated state,  $\text{Na}_v1.2$  channels with a mutation

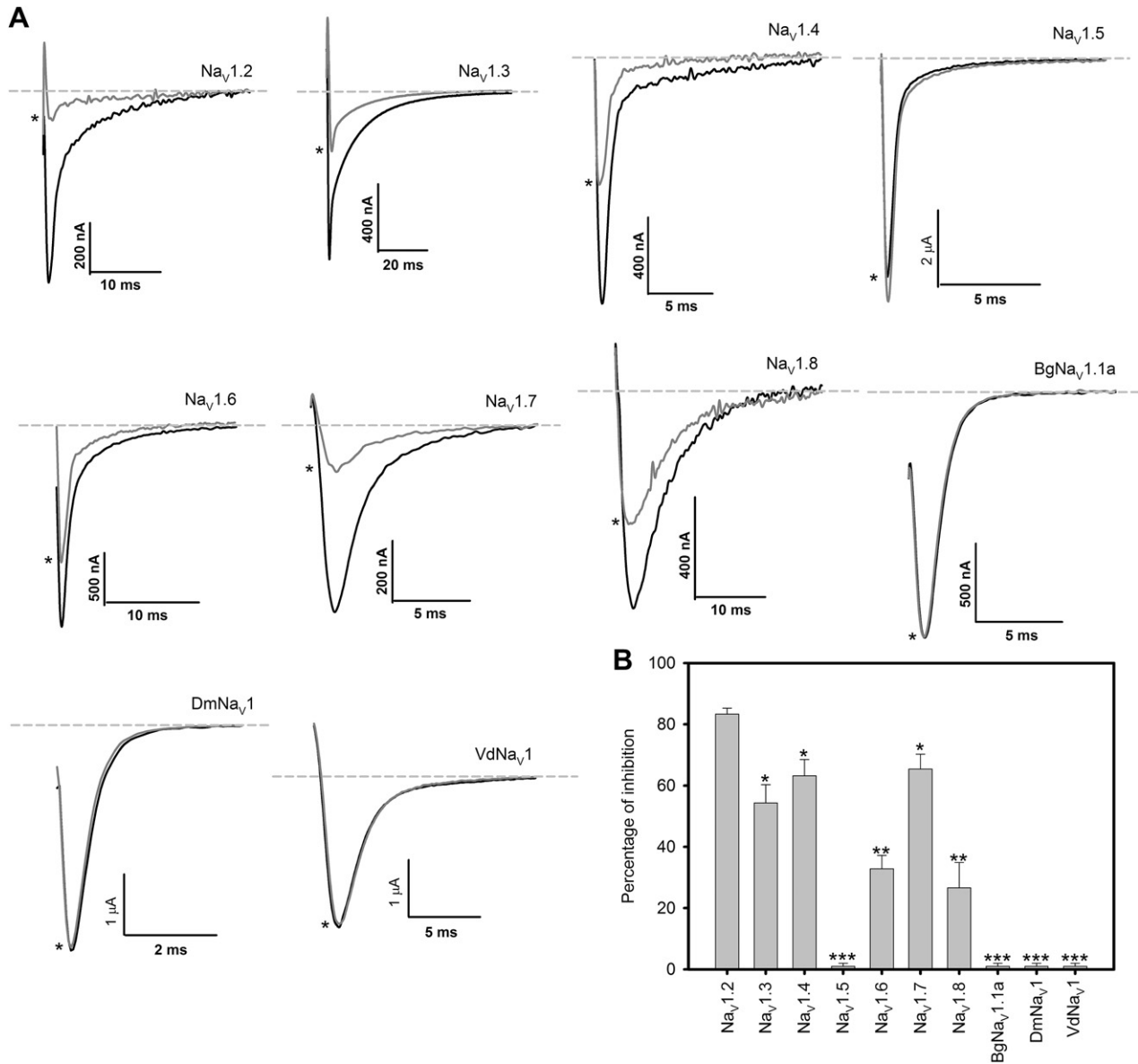


**Fig. 2.** Effect of rPnTx1 on different subtypes of sodium channels expressed in oocytes. (A) Representative records of Na<sup>+</sup> currents before (black line) and after (gray line\*) the addition of 1 μM rPnTx1. Dashed line is the baseline. Holding potential: −90 mV. Test potential: 0 mV. (B) Average percentage of Na<sup>+</sup> current inhibition by rPnTx1 (1 μM) of different sodium channel subtypes expressed in oocytes. Na<sub>v</sub>1.2 inhibition was significantly higher when compared with Na<sub>v</sub>1.3, Na<sub>v</sub>1.4 and Na<sub>v</sub>1.7 and these were higher when compared with Na<sub>v</sub>1.6 and Na<sub>v</sub>1.8. No effect was observed with Na<sub>v</sub>1.5 and with the arthropod isoforms (DmNa<sub>v</sub>1, BgNa<sub>v</sub>1.1a and VdNa<sub>v</sub>1). The symbols (\*), (\*\*) and (\*\*\*) denote the isoforms on which the toxin effects were not statistically different.

on the inactivation gate IFM/QQQ were used (Fig. 5). The current records in both control and experimental conditions showed sodium currents devoid of fast inactivation, and the inhibitory effect of 1 μM rPnTx1 can be clearly seen (74.0 ± 3.0% inhibition,  $n = 3$ ), although a little smaller than that observed with Na<sub>v</sub>1.2 channels without mutation (Fig. 4).

### 3.6. Effect of rPnTx1 in calcium channels present in DRG neurons

The amino acid sequence of PnTx1 has a similarity with the amino acid sequence of ω-agatoxin IIIA, which blocks calcium channels [5]. Previous articles suggested an effect of PnTx1 on neuronal calcium channels [9,10]. Martin-Moutot and colleagues [8] suggested that this effect is due a contamination with PnTx3-3, a toxin of *P. nigriventer* reported to be a potent inhibitor of calcium

channels [11]. The recombinant toxin provides an interesting opportunity to solve the issue, since it is produced in a heterologous system free from contamination with other toxins. Fig. 6 shows that 1 μM rPnTx1 does not alter significantly the calcium current of DRG, suggesting that this toxin is not promiscuous.

## 4. Discussion

The present article is the first electrophysiological study to characterize the effect and selectivity of the recombinant toxin rPnTx1 on different Na<sub>v</sub> channel isoforms. The experiments were carried out both on constitutively expressed sodium channels of DRG neurons and on isoforms expressed in *Xenopus* oocytes. DRG neurons express both TTX-S and TTX-R channels [15,16] and the latter proved to be less sensitive to rPnTx1. The recombinant toxin

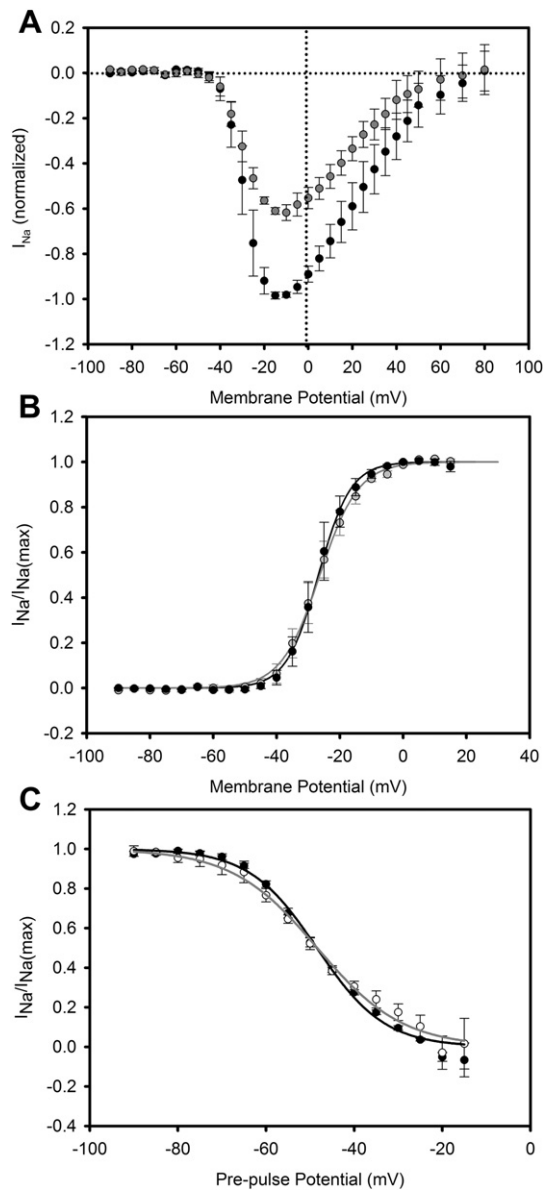


**Fig. 3.** Kinetic analysis of Nav1.2 inhibition. (A) Effect of rPnTx1 on the Na<sup>+</sup> current–voltage relationship before (black symbols) and after (gray symbols) the addition of 1  $\mu$ M rPnTx1. Average  $\pm$  SEM of 3 paired experiments. All values are normalized to the maximum peak current of the corresponding cell. (B) Effect of rPnTx1 on the voltage-dependence of activation before (black symbols) and after (gray symbols) the addition of 50 nM rPnTx1. Average  $\pm$  SEM of 5 paired experiments. The data were fitted with the Boltzmann equation (Material and methods), with the best fits of  $V_g = -26.78 \pm 0.28$  mV and  $-26.32 \pm 0.43$  mV,  $k_g = 5.11 \pm 0.25$  and  $6.11 \pm 0.38$ , for control and experimental, respectively. (C) Voltage-dependence of the steady-state inactivation before (black symbols) and after (gray symbols) the addition of 50 nM rPnTx1. Average  $\pm$  SEM of 3 paired experiments. The data were fitted with the Boltzmann equation (Material and methods), with the best fits of:  $V_h = -48.47 \pm 0.51$  and  $-48.37 \pm 0.54$  mV,  $k_h = 7.6 \pm 0.45$  and  $9.7 \pm 0.5$ , for control and experimental, respectively.

had no significant effect on calcium currents of DRG neurons, which strongly supports the interpretation that the previously reported effect on this type of channel was due to the contamination of the purified toxin with a calcium selective toxin [8].

Although native toxins are important tools to investigate ion channels, the possibility of expressing recombinant toxins has several important advantages, such as the possibility of having larger amount of material without contamination with different

toxins and, more importantly, the possibility of making well designed mutations in order to carry out structure–function studies and alter the toxin properties. The major difficulty to overcome is obtaining the correct folding of the recombinant toxin and the same activity as the native one. This is especially difficult with spider toxins, particularly with *P. nigriventer* toxins, that have high proportion of cysteines forming disulfide bridges [4]. In most attempts to express these toxins they came out with low or no activity. The expression of rPnTx1 is an important achievement, since it is a large (81 amino acids) peptide, with 7 disulfide bonds, as inferred by the comparison of its formula weight (8872.25 Da) and the measured molecular mass (8858.10 Da). Despite these difficulties, our results show that the recombinant toxin has even slightly higher affinity than the native one on Nav1.2 channels, as shown in Fig. 4. Due to the very limited amount of PnTx1, it was not possible to carry out structural comparisons.

Even more appealing is the observation that rPnTx1 shows a significant selectivity toward neuronal sodium channels. The following order of rPnTx1 sensitivity was obtained:  $rNav_{1.2} > rNav_{1.7} \approx rNav_{1.4} \geq rNav_{1.3} > mNav_{1.6} \geq hNav_{1.8}$ . No significant effect was seen on the cardiac Nav1.5. Similarly, it had no activity on arthropod channels. Of great interest is its high selectivity toward Nav1.7 channels, because of its involvement in acute and inflammatory pain [17]. The higher affinity to the Nav1.2 subtype was also observed with the  $\mu$ -conotoxins KIIIA (*Conus kinoshitai*) [18] and SIIIA (*Conus striatus*) [19]. By comparing the sequence of both toxins, one can observe an important similarity of the conotoxin KIIIA with a central segment of PnTx1 (Fig. 7). In fact, we can identify a sequence containing the amino acids W33, R35 and K39 that align with similar amino acids W8, R10 and R14, respectively, present in the  $\mu$ -conotoxin KIIIA [20,21]. Single mutations can alter significantly the selectivity of a toxin. The substitution tryptophan at position 8 by arginine decreased affinity of  $\mu$ -conotoxin KIIIA for Nav1.2 subtype, making it more selective to Nav1.4 [22]. Nonetheless, many structural questions about rPnTx1 remain open, which makes it an attractive object for further investigation.

Functional and competition experiments have characterized six toxin binding sites on sodium channels [2,3]. TTX and  $\mu$ -conotoxins, compete for the same site (site 1) and cause a blockage of the sodium channel pore. In the work published by Martin-Moutot and colleagues [8], binding experiments showed that PnTx1 competed with the  $\mu$ -conotoxin GIIIB and not with TTX. TTX competes with the conotoxin, which loses its ability to displace PnTx1 in the presence of excess of TTX. This means that PnTx1 and the  $\mu$ -conotoxins have different but overlapping sites.

The possibility that PnTx1 inhibits Na<sup>+</sup> currents by altering gating mechanisms was especially important to be considered since the effects of PnTx1 are more pronounced at depolarized holding potentials [8], what is also seen with the recombinant toxin (Fig. 1). One possible mechanism could be the stabilization of the inactivated state. The experiment in Fig. 5 shows that rPnTx1 markedly inhibits sodium channels devoid of fast inactivation, thus excluding the possibility of stabilizing the fast inactivated state.

Another feature of rPnTx1 that is similar to  $\mu$ -conotoxins KIIIA and GIIIA is the fact that the inhibition is not complete even at saturating concentrations. Fig. 4 shows that the maximal inhibition of Nav1.2 channels is 85.0% and 83.3% for the native and recombinant toxins, respectively. Since the Nav1.2 channels expressed consist of homogenous populations, it means that the inhibition of each channel is incomplete. This could happen by the decrease of single channel conductance or by alteration of gating kinetics. The voltage-dependences of activation and steady-state inactivation of sodium currents are not altered by the recombinant toxins, which makes it unlikely that the gating and open time probability are

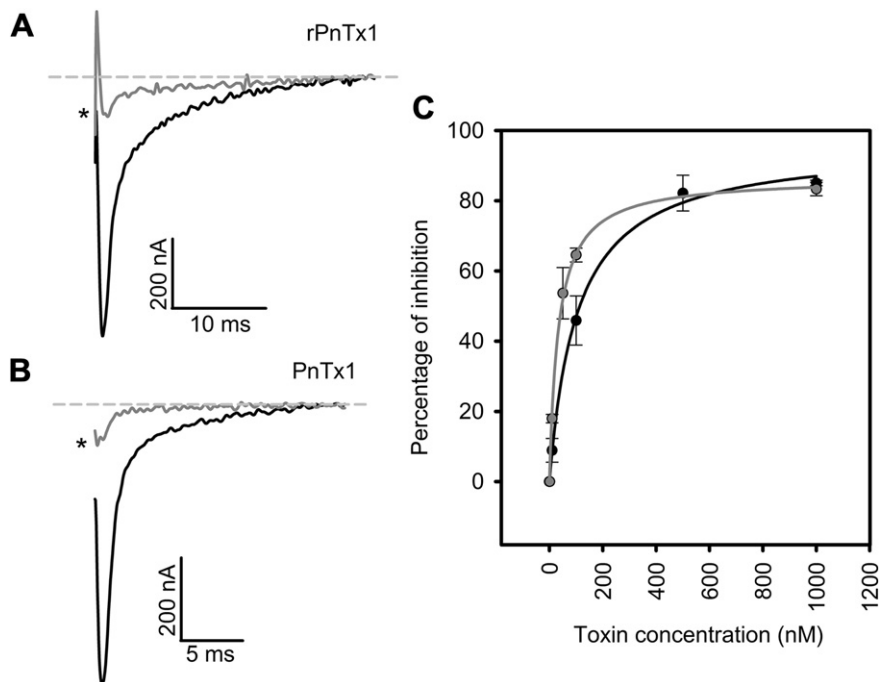


**Fig. 4.** Comparison of the effects of rPnTx1 and the purified PnTx1 on Nav1.2 channels. (A) Representative trace of the currents before (black) and after (gray\*) the addition of 1  $\mu$ M rPnTx1. (B) Representative trace of the currents before (black) and after (gray\*) the addition of 1  $\mu$ M PnTx1. (C) Concentration-dependence of the effect of PnTx1 (black symbols) and rPnTx1 (gray symbols). The data were fitted with the quadratic equation shown in Material and methods. Best fits were achieved with  $\max = 85.0 \pm 0.8\%$  and  $83.3 \pm 1.9\%$ ,  $IC_{50} = 105 \pm 12$  nM and  $33.7 \pm 2.9$  nM for PnTx1 and rPnTx1, respectively.

altered by the toxins (Fig. 3). Additionally, PnTx1 was shown not to compete with toxins that modify sodium channel gating [9], such as  $\alpha$ -scorpion toxins (site 3) and  $\beta$ -scorpion toxins (site 4) [23–25].

A likely mechanism of action is that it reduces the single channel conductance, in a manner similar to that shown for  $\mu$ -conotoxin GIIIA [26] and KIIIA [18], which bind to site 1. Furthermore, experiments show that TTX is able to bind to the channel even in the presence of  $\mu$ -conotoxins KIIIA, leading to complete inhibition of residual sodium current [27]. A model has been proposed that can account for these observations, based on the fact that these toxins are large compared to TTX. The model predicts that it can bind at the outer vestibule of the channel without its complete occlusion, thus allowing the channel to be activated but restricting the passage of  $Na^+$  ions [26–28]. It can also allow TTX to pass to its binding site, probably located deeper in the outer pore, thus causing its blockage. One can anticipate that mapping the sites of

interaction of *P. nigriventer* toxin will provide important insights into the toxin binding site and the structure of the channel outer vestibule [3]. The selectivity shown by rPnTx1 means that the outer region of the pore is not equal in all channel isoforms, and provide grounds for searching for more specific drugs.

The effect of depolarized holding potential remains to be clarified (Fig. 1D). A likely explanation is the alteration of its binding site as a consequence of the depolarized potential. This phenomenon may be of much interest, because the effect of PnTx1 will be more prominent on cells that remain depolarized longer times, which is invaluable in augmented activation of neurons, such as in neuropathic pain.

In fact, studies with the  $\mu$ -conotoxins previously mentioned, have shown that they have a potent analgesic effect [18,20]. This opens an interesting possibility to the use of rPnTx1. It is possible to perform assays with site directed mutations to make the toxin more specific to subtypes of sodium channels of interest. Thus the rPnTx1 becomes a promising tool for the development of

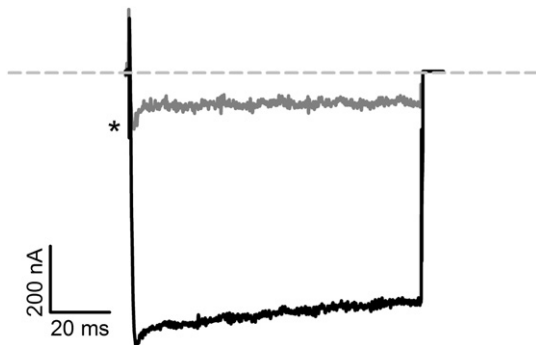


**Fig. 5.** Effect of rPnTx1 on Nav1.2 channels devoid of fast inactivation. Representative current records before (black) and after (gray\*) the addition of 1  $\mu$ M rPnTx1 to oocytes expressing Nav1.2 channels mutated to remove fast inactivation. The dashed line represents the baseline.

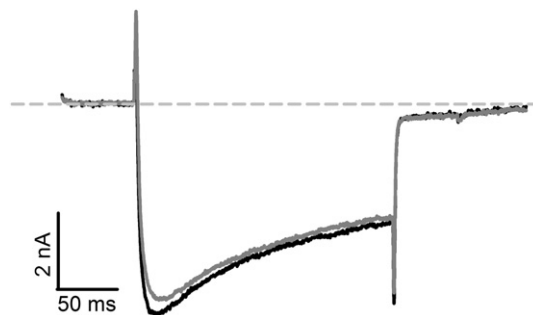


**Fig. 6.** Effect of rPnTx1 1  $\mu$ M on  $Ca^{2+}$  current of DRG neurons. Representative  $Ca^{2+}$  current recorded before (black) and 10 min after (gray\*) the addition of 1  $\mu$ M rPnTx1. The baseline is represented by the dashed line. The test pulse was  $-20$  mV for 200 ms.

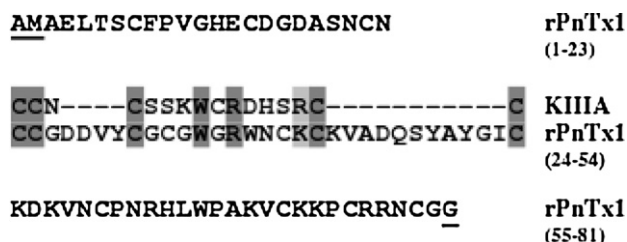


**Fig. 7.** Sequence alignment of rPnTx1 with KIIIA. Identical amino acids are highlighted with dark gray background and similar ones with light gray background. The three additional amino acids not present in the natural PnTx1 are underlined.

analgesics, or as model for new drugs. On the other hand, abnormal channel  $Na_v1.2$  expression is related with severe myoclonic epilepsy of infancy (Dravet syndrome), intractable childhood epilepsy with frequent generalized tonic-clonic seizures and benign familial neonatal-infantile seizures [29]. Patients with these diseases may benefit from drugs developed from rPnTx1 studies.

## 5. Conclusion

In this study we found that the rPnTx1 has similar effects as the native toxin PnTx1, with significant selectivity to the TTX-sensitive channels  $Na_v1.2$ ,  $Na_v1.7$ ,  $Na_v1.4$  and  $Na_v1.3$ , and no effect on isoform  $Na_v1.5$  and arthropod sodium channels. This toxin has a greater affinity to  $Na_v1.2$  subtype, with an  $IC_{50}$  of 33 nM. Since there are a number of channelopathies involving these channels, the expression of rPnTx1 opens a new perspective for understanding specific characteristics of the channel and the development of new drugs.

## Acknowledgments

The authors are indebted to Dr. Marta N. Cordeiro and Dr. M. E. de Lima for providing a sample of highly purified PnTx1. We are grateful to the following researchers for generously providing the following DNA clones: J. N. Wood (r $Na_v1.8$ ), A.L. Goldin (r $Na_v1.2$ , r $Na_v1.3$  and m $Na_v1.6$ ), G. Mandel (r $Na_v1.4$ ), R.G. Kallen (h $Na_v1.5$ ), K. Dong (Bg $Na_v1.1$  and Vd $Na_v1$ ), S.H. Heinemann (rat $\beta 1$  subunit), S.C. Cannon (h $\beta 1$  subunit) and M. S. Williamson (Para and tipE clones). The  $Na_v1.7$  clone was kindly provided by Roche. PSLB was supported by CNPq grants 303385/2008-1 and 477089/2010-0. JT was supported by the following grants: G.0433.12 (F.W.O. Vlaanderen), IUAP 7/19 (Inter-University Attraction Poles Program, Belgian State, Belgian Science Policy) and OT/12/081 (KU Leuven). AOS is recipient of a PhD fellowship from the Brazilian Research Council (CNPq). Partial support from FAPEMIG to PSLB and to MRVD are acknowledged. The present work is part of the INCTTOX/CNPq.

## References

- [1] J. Ekberg, D.J. Adams, Neuronal voltage-gated sodium channel subtypes: key roles in inflammatory and neuropathic pain, *Int. J. Biochem. Cell. Biol.* 38 (2006) 2005–2010.
- [2] S. Cestèle, W.A. Catterall, Molecular mechanisms of neurotoxin action on voltage-gated sodium channels, *Biochimie* 82 (2000) 883–892.
- [3] W.A. Catterall, S. Cestèle, V. Yarov-Yarovsky, F.H. Yu, K. Konoki, T. Scheuer, Voltage-gated ion channels and gating modifier toxins, *Toxicon* 49 (2007) 124–141.
- [4] M.H. Borges, M.E. De Lima, M. Stankiewicz, M. Pelhate, M.N. Cordeiro, P.S.L. Beirão, Structural and functional diversity in the venom of spiders of the genus *Phoneutria*, in: M.E. De Lima, A.M.C. Pimenta, M.F. Martin-Eauclaire, R.B. Zingali (Eds.), *Animal Toxins: State of the Art Perspectives in Health and Biotechnology*, UFMG, Belo Horizonte, 2009, pp. 291–312.
- [5] M. Richardson, A.M.C. Pimenta, M.P. Bemquerer, M.M. Santoro, P.S.L. Beirão, M.E. Lima, S.G. Figueiredo, C. Bloch Jr., E.A.R. Vasconcelos, F.A.P. Campos, P.C. Gomes, M.N. Cordeiro, Comparison of the partial proteomes of the

- venoms of Brazilian spiders of the genus *Phoneutria*, *Comp. Biochem. Physiol.* 142 (2006) 173–187.
- [6] M.R.V. Diniz, R.D.G. Theakston, J.M. Crampton, M.N. Cordeiro, A.M.C. Pimenta, M.E. De Lima, C.R. Diniz, Functional expression and purification of recombinant Tx1, a sodium channel blocker neurotoxin from the venom of the Brazilian “armed” spider, *Phoneutria nigriventer*, *Protein Expr. Purif.* 50 (2006) 18–24.
- [7] C.R. Diniz, M.N. Cordeiro, L.R. Juno, P. Kelly, S. Fischerj, F. Reimann, E.B. Oliveira, M. Richardson, The purification and amino acid sequence of the lethal neurotoxin Tx1 from the venom of the Brazilian ‘armed’ spider *Phoneutria nigriventer*, *FEBS J.* 263 (1990) 251–253.
- [8] N. Martin-Moutot, P. Mansuelle, G. Alcaraz, R. Gouvêa Dos Santos, M.N. Cordeiro, M.E. De Lima, M. Seagar, C. Van Renterghem, *Phoneutria nigriventer* toxin 1: a novel, state-dependent inhibitor of neuronal sodium channels that interacts with  $\mu$ -conotoxin binding sites, *Mol. Pharmacol.* 69 (2006) 1931–1937.
- [9] R.G. Santos, C.R. Diniz, M.N. Cordeiro, M.E. De Lima, Binding sites and actions of Tx1, a neurotoxin from the venom of the spider *Phoneutria nigriventer*, in guinea pig ileum, *Braz. J. Med. Biol. Res.* 32 (1999) 1565–1569.
- [10] R. Gouvêa dos Santos, M.A. Soares, J.S. Cruz, R. Mafra, R. Lomeo, M.N. Cordeiro, A.M. Pimenta, M.E. De Lima, Tx1, from *Phoneutria nigriventer* spider venom, interacts with dihydropyridine sensitive-calcium channels in GH3 cells, *J. Radioanal. Nucl. Chem.* 269 (2006) 585–589.
- [11] R.M. Leão, J.S. Cruz, C.R. Diniz, M.N. Cordeiro, P.S.L. Beirão, Inhibition of neuronal high-voltage activated calcium channels by the  $\omega$ -*Phoneutria nigriventer* Tx3-3 peptide toxin, *Neuropharmacology* 39 (2000) 1756–1767.
- [12] F.S. Torres, C.N. Silva, L.F. Lanza, A.V. Santos, A.M.C. Pimenta, M.E. De Lima, M.R.V. Diniz, Functional expression of a recombinant toxin – rPnTx2-6 – active in erectile function in rat, *Toxicon* 56 (2010) 1172–1180.
- [13] F. Sanger, S. Nicklen, A.R. Coulson, DNA sequencing with chain-terminating inhibitors, *Proc. Natl. Acad. Sci. U. S. A.* 74 (1977) 5463–5667.
- [14] E.R. Moraes, E. Kalapothakis, L.A. Naves, C. Kushmerick, Differential effects of *Tityus bahiensis* scorpion venom on tetrodotoxin-sensitive and tetrodotoxin-resistant sodium currents, *Neurotoxin. Res.* 19 (2011) 102–114.
- [15] C. Ho, M.E. O’Leary, Single-cell analysis of sodium channel expression in dorsal root ganglion neurons, molecular and cellular neuroscience, *Mol. Cell. Neurosci.* 46 (2011) 159–166.
- [16] R.M. Brochu, I.E. Dick, J.W. Tarpley, E. McGowan, D. Gunner, J. Herrington, P.P. Shao, D. Ok, C. Li, W.H. Parsons, G.L. Stump, C.P. Regan, J.J. Lynch Jr., K.A. Lyons, O.B. McManus, S. Clark, Z. Ali, G.J. Kaczorowski, W.J. Martin, B.T. Priest, Block of peripheral nerve sodium channels selectively inhibits features of neuropathic pain in rats, *Mol. Pharmacol.* 69 (2006) 823–832.
- [17] M. Liu, J.N. Wood, The roles of sodium channels in nociception: implications for mechanisms of neuropathic pain, *Pain Med.* 12 (2011) S93–S99.
- [18] M.-M. Zhang, B.R. Green, P. Catlin, B. Fiedler, L. Azam, A. Chadwick, H. Terlau, J.R. McArthur, R.J. French, J. Gulyas, J.E. Rivier, B.J. Smith, R.S. Norton, B.M. Olivera, D. Yoshikami, G. Bulaj, Structure/function characterization of  $\mu$ -conotoxin KIIIA, an analgesic, nearly irreversible blocker of mammalian neuronal sodium channels, *J. Biol. Chem.* 282 (2007) 30699–30706.
- [19] S. Yao, M.-M. Zhang, D. Yoshikami, L. Azam, B.M. Olivera, G. Bulaj, R.S. Norton, Structure, dynamics, and selectivity of the sodium channel blocker  $\mu$ -conotoxin SIIIA, *Biochem. J.* 47 (2008) 10940–10949.
- [20] K.K. Khoo, Z.-P. Feng, B.J. Smith, M.-M. Zhang, D. Yoshikami, B.M. Olivera, G. Bulaj, R.S. Norton, Structure of the analgesic  $\mu$ -conotoxin KIIIA and effects on the structure and function of disulfide deletion, *Biochem. J.* 48 (2009) 1210–1219.
- [21] M.-M. Zhang, T.S. Han, B.M. Olivera, G. Bulaj, D. Yoshikami,  $\mu$ -Conotoxin KIIIA derivatives with divergent affinities versus efficacies in blocking voltage-gated sodium channels, *Biochem. J.* 49 (2010) 4804–4812.
- [22] A. Van Der Haegen, S. Peigneur, J. Tytgat, Importance of position 8 in  $\mu$ -conotoxin KIIIA for voltage gated sodium channel selectivity, *FEBS J.* 278 (2011) 3408–3418.
- [23] W.A. Catterall, Neurotoxins that act on voltage-sensitive sodium channels in excitable membranes, *Ann. Rev. Pharmacol. Toxicol.* 20 (1980) 15–43.
- [24] F.V. Campos, B. Chanda, P.S.L. Beirão, F. Bezanilla,  $\alpha$ -Scorpion toxin impairs a conformational change that leads to fast inactivation of muscle sodium channels, *J. Gen. Physiol.* 132 (2008) 251–263.
- [25] F.V. Campos, B. Chanda, P.S.L. Beirão, F. Bezanilla,  $\beta$ -Scorpion toxin modifies gating transitions in all four voltage sensors of the sodium channel, *J. Gen. Physiol.* 130 (2007) 257–268.
- [26] R.J. French, E. Prusak-Sochaczewski, G.W. Zamponi, S. Becker, A.S. Kularatna, R. Horn, Interactions between a pore-blocking peptide and the voltage sensor of the sodium channel: an electrostatic approach to channel geometry, *Neuron* 16 (1996) 407–413.
- [27] M.-M. Zhang, J.R. McArthur, L. Azam, G. Bulaj, B.M. Olivera, R.J. French, D. Yoshikami, Synergistic and antagonistic interactions between tetrodotoxina and  $\mu$ -conotoxin in blocking voltage-gated sodium channels, *Channels* 3 (2009) 32–38.
- [28] R.J. French, D. Yoshikami, M.F. Sheets, B.M. Olivera, The tetrodotoxin receptor of voltage-gated sodium channels—perspectives from interactions with  $\mu$ -conotoxins, *Mar. Drugs* 8 (2010) 2153–2161.
- [29] A.L. George Jr., Inherited disorders of voltage-gated sodium channels, *J. Clin. Invest.* 115 (2005) 1990–1999.